

Design Optimization of Plug-in Hybrid Electric Vehicles

Biswajit Barik, Sohan Ram Choudhary, Adnan Patel, Dara Shyam Sundar, Saurav Mahapatra, Dr. Prasad Krishna

Abstract— Today's era of transportation has touched new frontiers with the advancement of technology compelling humanity to strive harder to achieve a better solution towards a greener and sustainable power source in automobiles. With the fossil fuels depleting at an accelerated rate, electrical energy has emerged to be an alternative for the propulsion system in automobiles. Since vehicles powered solely by electrical energy do not meet the performance standards, a Hybrid Electric Vehicle (HEV) is developed which combines both electric and conventional petrol combustion system, hence enhancing the fuel economy, reducing the carbon emissions and improving performance. With the right amount of proportioning between the two energy sources, this field has become one of the most significant research areas in the current decade. The present work involves geometric modelling and computational fluid dynamics (CFD) analysis of the chassis, simulation of the power-split drive-train configuration on LABVIEW and demonstration of toggling between the two energy sources on a PHEV prototype. The CFD analysis gives the velocity variation and pressure distribution over the vehicle, thus streamlining the chassis to minimize the drag coefficient and the rolling resistance.

Index Terms— Hybrid Electric Vehicles, CFD, Pressure Distribution, Velocity Distribution, Drag Coefficient, Rolling Resistance.

1 INTRODUCTION

The objective of this work is to design and analyze a Plug-in Hybrid Electric Vehicle (PHEV). The hunt for Environmental-friendly vehicles has been on for a while now. Although alternative sources of fuel such as biodiesel and hydrogen may reduce emissions from internal combustion engines, they are not available in sufficient quantities. Electrical vehicles though have no emissions, but have a limited range and the batteries take a long time to recharge. [6], [10]

To overcome this drawback of an electric vehicle, a PHEV was conceived. Besides reducing emissions, it offers increased mileage and comfortable driving experience. Hybrid vehicles feature a power train that includes a traditional internal combustion engine as well as an electric motor, a battery and a generator. [9], [12]

PHEV vehicle architecture consists of an electric drive train and a drive-train powered by an internal combustion engine that is coupled with each other by a power-split hybrid configuration. The power generated by the engine charges the battery and runs the vehicle through a planetary gear set for toggling through the gear ratios. Energy stored in the battery runs the generator at low speed conditions. [2], [3], [4]

The PHEV vehicle should have a minimum drag coefficient, ranging from 0.4 to 0.9, to minimize the aerodynamic drag

force and rolling resistance, while the vehicle is in motion. Since the vehicle is initially powered by an electrical power source, which is considerably less than the power provided by a fuel powered engine, the profile should be aerodynamically designed in an efficient way to improve the energy utilization and the economy of the vehicle. [5], [15]

2 DESIGN OF PHEV

2.1 Design of Chassis

A geometric model of the chassis was created in CATIA V5 as shown in Fig 1. This model was exported to ANSYS workbench for the CFD analysis.

2.2 Design of PHEV prototype

The PHEV vehicle was designed from an existing remote controlled car (RC 6197 TOMAHAWK) with a 1/10scale nitro-powered engine. The base of the car as rebuilt to adjust the electrical parts (i.e. d.c. motor and battery), as shown in Fig 2. The front differential and the axle was replaced by a 12 V dc motor of 500 rpm (torque of 18 kg-cm) was coupled to the front wheel.

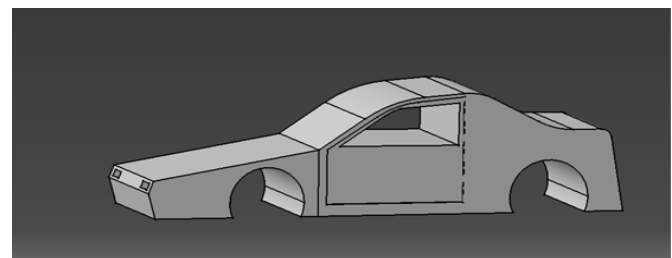


Fig 1 : CATIA model of the Chassis

- Biswajit Barik, Department of Mechanical Engineering, National Institute of Technology, Surathkal. E-mail: biswajitbarik90@gmail.com
- Sohan Ram Choudhary, Department of Mechanical Engineering, National Institute of Technology, Surathkal. E-mail: sohan.nitk@gmail.com
- Adnan Patel, Department of Mechanical Engineering, National Institute of Technology, Surathkal. E-mail: adnanpatel06@gmail.com
- Dara Shyam Sundar, Department of Mechanical Engineering, National Institute of Technology, Surathkal. E-mail: ssdara49@gmail.com
- Saurav Mahapatra, Department of Mechanical Engineering, National Institute of Technology, Surathkal. E-mail: rishi7910@gmail.com
- Dr. Prasad Krishna, Head of Department of Mechanical Engineering, National Institute of Technology, Surathkal. E-mail: krishnprasad@gmail.com

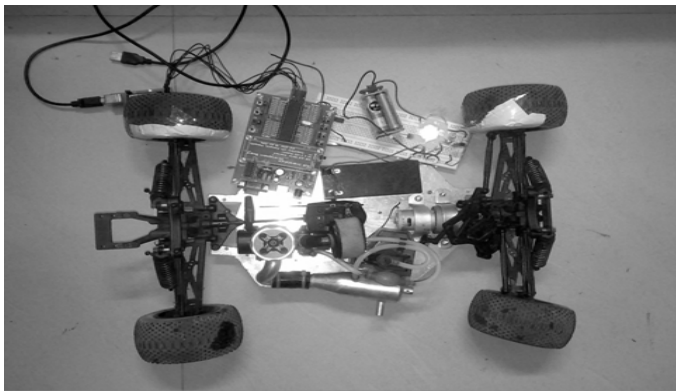


Fig 2: The PHEV prototype drivetrain

A MR1212 Lead-Acid rechargeable battery (12 V, 1.2 Ah) was placed alongside the motor so that the center of gravity of the vehicle would not be disturbed significantly. The microcontrollers and sensors for toggling were placed on top of the battery in safe conditions. The maximum speed of wheel was 5,000 rpm, approximately 12 m/s and the toggling is initially set at 300 rpm.

The sensor circuit, shown in Fig 3, consisted of an IR (infra red) LED (light-emitting diode), a photo resistor, a variable resistor of 10 kΩ and a 330 Ω resistor. The circuit was powered by a 5 V supply. The IR LED senses the interruption occurring due to the rotational movement of the wheel and converts it into the rotational speed. The circuit disconnects the power drawn from the battery and starts the IC engine at speed greater than 300 rpm and reconnects it to the battery when speed falls below 300 rpm.

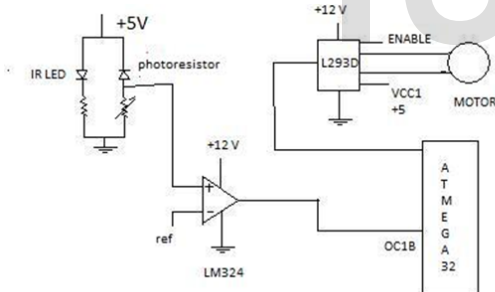


Fig 3: Layout of the electric components

3 CFD ANALYSIS F THE CHASSIS

3.1 Defining the domain

A rectangular box (wind tunnel) was created enclosing the chassis with one of its face coinciding with the later. This plane of coincidence was the symmetrical plane denoted by 'sym'. Using Boolean operations the sub-domain of the car was subtracted from the larger domain which resulted in creation of the required model suitable for analysis. The regions of inlet, outlet and the boundary faces were defined as shown along with the direction of flow of fluid. The wall facing the viewer is the sym wall. The top, bottom and side walls are the boundary walls.

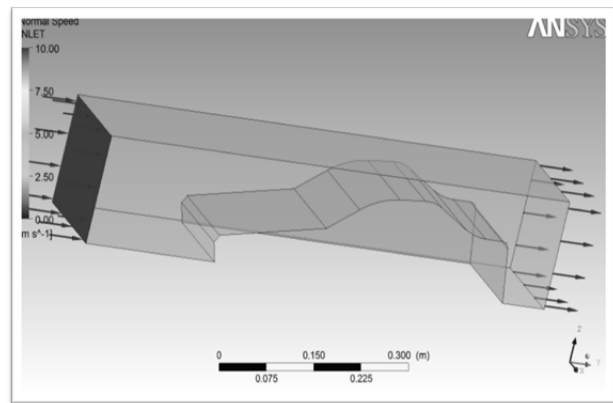


Fig 4: Domain created in ANSYS with boundary conditions

3.2 Meshing

The mesh of the domain was generated of tetrahedron geometry with minimum size of 0.01 mm. The quality of meshing determines the accuracy of the results obtained. Volumetric mesh of the domain created was obtained to simulate the flow.

3.3 Establishing boundary conditions

The pressure was set to 0. Ideal movement speed of the Vehicle was assumed to be 10 m/s. So the relative air flow was assumed to be the same flowing against the vehicle. The flow was analyzed at ambient conditions of air. The flow was made laminar in nature. The CFX solver was executed to analyze the flow. Fig 4 shows the domain obtained after the chassis is subtracted from the wind tunnel in shape of cuboids and the boundary conditions applied.

4 SIMULATION OF THE POWER-SPLIT DRIVE TRAIN CONFIGURATION

The energy flow in a typical PHEV was simulated in LABVIEW. The power above certain limits is provided by the IC engine, which is a function of velocity in this model. At lower speeds, power is supplied by the battery. Regeneration takes place when brakes are applied. Arrow marks are used to give the direction of energy flow which was built by Boolean LEDs.

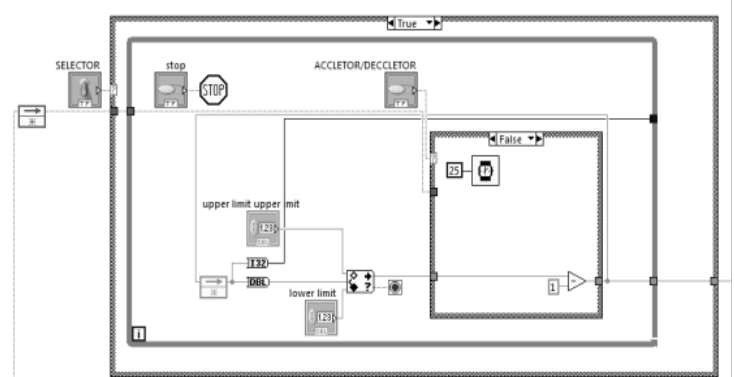


Fig 5: Front panel showing case statement for acceleration And deceleration

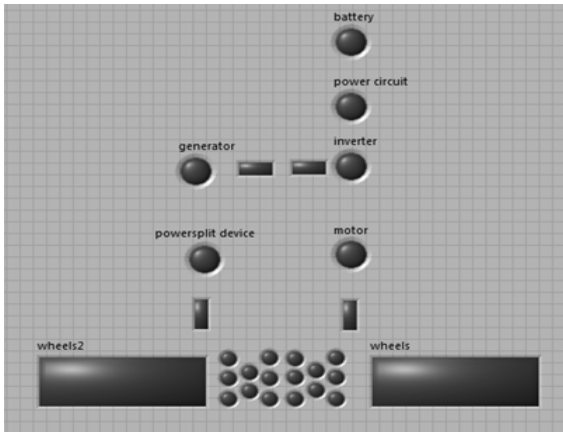


Figure 6: Main window of LABVIEW indicating different components in PHEV

The direction of arrow changes when brakes are applied to indicate the reverse flow of energy from wheels to battery. A while loop is used to achieve the continuous change in velocity till the required speed is achieved. This is achieved by placing LEDs. If it is accelerating, the condition is true; then instead of decrement the increment operator is operated in the case loop within the while condition. The wait operator is used to specify how many milliseconds one needs to wait before executing the next calculation. It results in continuous acceleration/deceleration of the vehicle till required speed is achieved. In this way, variation of velocity over the time is achieved.

Upper limit and lower limit is to be specified by the user so that velocity is varied between two limits. In Range and Coerce function is used to coerce the values between the specified ranges so that velocity is varied between the ranges. If an overflow occurs, it chooses the upper limit; and if a value lesser than the lower limit is given, then it chooses the limit.

LABVIEW is used to demonstrate the power flow in vehicle during the following conditions. Fig 5 and 6 shows the front panel and main window for created to simulate the drivetrain.

1) Low Speeds: Here low speed means 0-300 rpm. The flow of energy is downwards and towards the wheels. Energy is supplied from battery to wheels via power circuit, inverter and motor. So accordingly the corresponding LEDs go to higher states. It is achieved by using comparator; if velocity is in the range of 0-300 rpm, then they go to ON state.

2) High Speeds: This occurs for speeds greater than 300 rpm. Energy flow is same as in earlier case but now power comes from engine to wheels via power-split device to generator and inverter and it runs the motor which drives the wheels. This state is done whenever velocity is greater than 300 rpm and brake is in OFF state.

3) Regeneration: It means recovering the kinetic energy which would otherwise be lost in the form of heat. It works when brakes are applied. So flow of energy is from wheels to battery via motor, inverter and power circuit. So the direction is reversed and accordingly LEDs go to higher state as explained earlier.

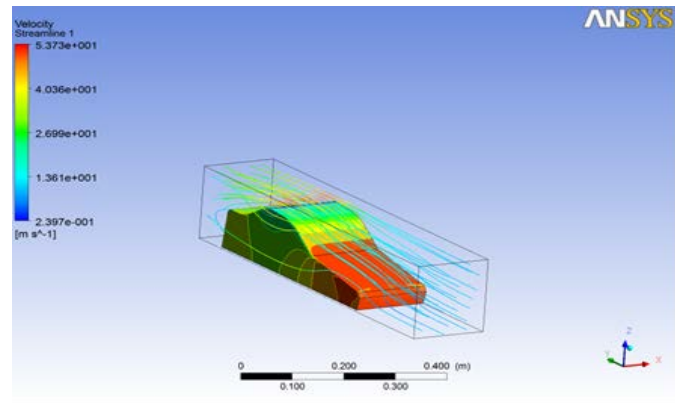


Fig 7: Flow analysis showing the turbulence of air flow and the pressure contours

4) Charging: In the present model charging is done while in rest condition, i.e. velocity is zero. Here energy flows upward from engine to battery via power-split device. LEDs are used to indicate the current status of battery, whether it is charging or running on battery or regeneration.

5 RESULTS AND DISCUSSIONS

The laminar airflow and the pressure contour over the chassis by the finite element analysis were generated as shown in the Fig 7. It was observed that most of the flow lines accumulated at the roof of the car on a minimal area. The gradient of the streamlines represented the level of turbulence gained during the flow over the chassis.

The pressure builds up heavily near the bonnet of the chassis which subsequently decreases towards the hood. The streamlined airflow grew turbulent as it approached the wind-shield and top domain of the car.

During the working of the HEV prototype, when the power was given to the microcontroller, the LED's lit up and the wheels rotated signifying the power was drawn from the battery and the car was driven by electric propulsion. On reaching a particular speed limit, toggling action takes place resulting in shutting down of battery power and subsequently powering up of the engine by fuel power. Once the speed lowers below the threshold set at 300 rpm, the toggling action takes place.

The power drawn when the vehicle operates on battery was calculated by the following formulae.

$$\text{Power} = \text{Voltage} \times \text{current rating} \quad (1)$$

Where,

Voltage = 12 volts and

Current = 1.2 Ampere hour

Power = 14.4 Watt hour

The power drawn when the vehicle operates on fuel was calculated by the formulae:

$$\text{Power} = 2\pi \times N \times T \times m / 60 \quad (2)$$

Where,

N = speed of the vehicle = 300 rpm

T = torque of the vehicle = 3kg-cm

m = Number of cylinders = 1

Power = 9.24 Watt hour

Since the toggling action takes place at 300 rpm, a jerking motion is produced due to the difference in power drawn from the two energy sources. A number of iterations were done to dampen the jerking motion. It was found that at speed 350 rpm, the jerking produced due to the power difference was minimized.

Aerodynamic drag

$$F_D = 0.5 \times \rho_a \times V_{rel}^2 \times C_D(\phi) \times A(\phi) \quad (3)$$

Where:

F_D	aerodynamic drag force [N]
ρ_a	air density [Kg/m ³]
V_{rel}	relative velocity of vehicle [m/s]
C_D	aerodynamic drag coefficient
A	cross sectional area exposed to wind [m ²]
ϕ	wind yaw angle [rad]

Average value of drag pressure obtained from the ANSYS solver CFX = 400 Pa.

Equivalent drag force obtained (F_D) = 93 N.

Net cross-sectional area contributing to the drag = 1.518 m²

Density of air (ρ_a) = 1.3 kg m⁻³

Substituting the values into (3),

$$C_D = 0.943$$

Rolling resistance

$$F_{rr} = m_{veh} \times g \times \mu \quad (4)$$

Where:

F_{rr}	Rolling resistance force [N]
m_{veh}	Vehicle mass [Kg]
g	Gravitational constant [m/s ²]
μ	Rolling resistance coefficient (RRC)

The value of rolling resistance coefficient (RRC) of tires = 0.0062

Mass of vehicle = 4.1 kg

Substituting the values into equation,

$$F_{rr} = 0.249 \text{ N}$$

The aerodynamic Drag coefficient was found to be 0.943 which was quite higher as compared to the required values between 0.4 - 0.9. The Rolling Resistance force could be minimized by redesigning the tires and reducing the weight of the vehicle.

5 CONCLUSIONS

Following are the concluded from the present work:

- 1) The CFD analysis of the chassis represented a uniformly distributed pressure gradient over the chassis of the vehicle. Hence the structural stability of the bonnet should be emphasized upon to withstand high pressure while taking care of the net power to weight ratio.
- 2) The turbulent eddies formed at the roof could be minimised by redesigning the chassis of the car.
- 3) The value of the drag coefficient was found to be 0.943. The rolling resistance force was found to be 0.249 N which can be reduced to increase the overall efficiency.
- 4) The PHEV prototype built on an RC car demonstrated

the toggling between the two energy sources.

- 5) More effective approaches in a PHEV are possible by developing appropriate software and hardware based on the situations and market conditions.

Further research may lead to evolution of more efficient technologies which may reduce the dependency on petrol and diesel leading to better fuel efficiency.

REFERENCES

- [1] Anjad S., Neelakrishnan S., Rudramoorthy R. (2010), "Review of design considerations and technological challenges for successful development and deployment of plug-in hybrid electric vehicles", *Renewable and Sustainable Energy Reviews* (14) 1104-1110.
- [2] Arce A., Bordons C., del Real A.J. (2009), "MPC for battery/fuel cell hybrid vehicles including fuel cell dynamics and battery performance improvement", *Journal of Process Control* (19) 1289-1304.
- [3] Banjac T., Katrašnik T., Trenc F. (2009), "Energy conversion efficiency of hybrid electric heavy-duty vehicles operating according to diverse drive cycles", *Energy Conversion and Management* (50) 2865-2878.
- [4] Bayindir K.C., Gozukucuk M.A., Teke A. (2011), "A comprehensive overview of hybrid electric vehicle: Powertrain configurations, powertrain control techniques and electronic control units", *Energy Conversion and Management* (52) 1305-1313.
- [5] Bradley T.H., Quinn C.W. (2010), "Analysis of plug-in hybrid electric vehicle utility factors", *Journal of Power Sources* (195) 5399-5408.
- [6] Bradley T.H., Frank A.A. (2009), "Design, demonstrations and sustainability impact assessments for plug-in hybrid electric vehicles", *Renewable and Sustainable Energy Reviews* (13) 115-128.
- [7] Chau K.T., Wong Y.S. (2002), "Overview of power management in hybrid electric vehicles", *Energy Conversion and Management* (43) 1953-1968.
- [8] Chen C.C., Huang K.D., Jeng T.M., Tzeng S.C. (2005), "Integration mechanism for a parallel hybrid vehicle system", *Applied Energy* (82) 133-147.
- [9] Chen Y.J., Hwang J.J., Kuo J.K. (2012), "The study on the power management system in a fuel cell hybrid vehicle", *International Journal of Hydrogen Energy* (37) 4476-4489.
- [10] Chowdhury M., He Y., Mac Y., Pisu P. (2012), "An energy optimization strategy for power-split drivetrain plug-in hybrid electric vehicles", *Transportation Research Part C* (22) 29-41.
- [11] Gao D., Li J., Lu L., Ouyang M., Xie Q., Xu L. (2006), "Performance comparison of two fuel cell hybrid buses with different powertrain and energy management strategies", *Journal of Power Sources* (163) 467-479.
- [12] Hirsh R.F., Sovacool B.K. (2009), "Beyond batteries: An examination of the benefits and barriers to plug-in hybrid electric vehicles (PHEVs) and a vehicle-to-grid (V2G) transition", *Energy Policy* (37) 1095-1103.
- [13] Li C.Y., Liu G.P. (2009), "Optimal fuzzy power control and management of fuel cell/battery hybrid vehicles", *Journal of Power Sources* (192) 525-533.
- [14] Katrašnik T. (2009), "Analytical framework for analyzing the energy conversion efficiency of different hybrid electric vehicle topologies", *Energy Conversion and Management* (50) 1924-1938.
- [15] Katrašnik T. (2007), "Hybridization of powertrain and downsizing of IC engine - analysis and parametric study", *Energy Conversion and Management* (48) 1424-1434.
- [16] Kim M.J., Peng H. (2007), "Power management and design optimization of fuel cell/battery hybrid vehicles", *Journal of Power Sources* (165) 819-832.